JOURNAL OF SOLID STATE CHEMISTRY 112, 307–311 (1994)

Structure of $Pb_7Sb_4S_{13}$, a Higher Homolog of Boulangerite

A. Skowron,[1] F. W. Boswell, J. M. Corbett, and N. J. Taylor*

*Guelph-Waterloo Program for Graduate Work in Physics, Waterloo Campus, Waterloo, Ontario, N2L 3G1 Canada; and *Department of Chemistry, University of Waterloo, Waterloo, Ontario, N2L 3G1 Canada*

Received March 15, 1993; in revised form December 1, 1993; accepted December 3, 1993

The structure of $Pb_7Sb_4S_{13}$ has been determined as orthorhombic, space group $P2_12_12_1$. $a = 23.488(3)$ Å, $b = 25.220(3)$ Å, $c = 4.0821(4)$ Å, $V = 2418.1(5)$ Å^3, $Z = 4$, $D_x = 6.466$ g/cm^3, Mo$K\alpha$ radiation, $\lambda = 0.71073$ Å, $\mu = 544.190$ cm^{-1}, $F(000) = 3944$, room temperature, $R = 0.064$, and $wR = 0.067$ for 2034 observed independent reflections. The crystal was prepared by synthesis in evacuated silica tubes at 898 K in the presence of I_2. $Pb_7Sb_4S_{13}$ is a higher homolog of boulangerite, $Pb_5Sb_4S_{11}$, with similar cation distribution, determined by the bond-valence method, but with a lower space group symmetry.

INTRODUCTION

Salanci (1) reported the synthesis of phase II, stable between 890 and 908 K and having a composition close to $Pb_7Sb_4S_{13}$. Here we report its structure determination, undertaken as a part of a broader study of the $PbS–Sb_2S_3$ system. The general aspects of the structural chemistry of lead–antimony sulfides are the subject of a separate report (2).

EXPERIMENTAL

Single crystals of $Pb_7Sb_4S_{13}$ were synthesized from elemental lead, antimony, and sulfur of "Specpure" grade supplied by Johnson Matthey plc. Four samples were prepared by weighing the elements in proportions corresponding to 81, 79, 76, and 74 mole% PbS. The samples were sealed in evacuated silica tubes, melted at 1150 K for 2 days, and then annealed at 773 K for 7 days. Separation of the ingots occurred in all the ampoules. Separate parts of ingots were ground to a fine powder, from which a total of eight pellets were made. Each pellet was placed in an approximately 20-cm-long silica tube together with 1 mg of I_2. The tubes were evacuated, sealed, and annealed in a two-zone horizontal furnace. The pellets were kept at the cooler end, at 898 K; the other end was 911 K. Needle-like crystals grew on the walls of the ampoules, typically 3–4 cm away from the pellets. A number of crystals were mounted with the needle axis, corresponding to the short crystallographic axis, normal to the geometer axis, and examined on a precession camera. In this way the two longer crystallographic axes could be measured and the crystals easily identified. Two types of crystals were found, typically both in one batch: $Pb_7Sb_4S_{13}$ and $Pb_3Sb_2S_6$. The latter were identified from the lattice parameters corresponding to those reported by Wang (3) but no untwinned crystal was found. A good quality, 0.04 × 0.052 × 0.64-mm crystal of $Pb_7Sb_4S_{13}$ was found in the batch corresponding to 74 mole% PbS.

A summary of the structure determination of $Pb_7Sb_4S_{13}$ is presented in Table 1. The absences, $h00{:}\,h = 2n + 1$, $0k0{:}k = 2n + 1$, and $00l : l = 2n + 1$, found by the precession method uniquely indicate the noncentrosymmetric space group $P2_12_12_1$. The structure refinement was carried out with anistropic atomic displacement parameters only for cations and mixed Pb and Sb occupancies for the cation sites. Due to strong correlations between the site occupation numbers and the atomic displacement parameters, the occupation numbers and the displacement parameters were refined alternatively until the best agreement indices were obtained. Occupancies were then fixed in the final cycle. Complex scattering factors for neutral atoms were taken from "International Tables for X-Ray Crystallography" (4).

The occupation numbers, used to generate the final atomic positions and the anisotropic thermal displacement parameters listed in Tables 2 and 3, are given in Table 4. The interatomic distances are listed in Table 5. The occupation numbers were also determined independently by the bond-valence method as described by Skowron and Brown (5). In this, the refined atomic coordinates were used to calculate the bond lengths (r) from which the valences (s) were calculated using the equation

$$s = \exp\left[(r_0 - r)/0.37\right], \qquad [1]$$

---

[1] To whom correspondence should be addressed.

0022-4596/94 $6.00

TABLE 1
Structure Determination Summary

	Crystal data
Empirical formula	$Pb_7Sb_4S_{13}$
Color; habit	Gray needle fragment
Crystal size (mm)	0.040{100} × 0.052{010} × 0.64{001}
Crystal system	Orthorhombic
Space group	$P2_12_12_1$
Unit cell dimensions	a = 23.488(3) Å; b = 25.220(3) Å; c = 4.0821(4) Å
Volume	2418.1(5) $Å^3$
Z	4
Formula weight	2354.1
Density (calc.)	6.466 g/gm^3
Absorption coefficient	544.19 cm^{-1}
$F(000)$	3944
	Data collection
Diffractometer used	Siemens R3m/V
Radiation	Mo$K\alpha$ (λ = 0.71073 Å)
Temperature (K)	295
Monochromator	Highly oriented graphite crystal
2θ range	4.0 to 56.0°
Scan type	ω
Scan speed	Variable; 1.50 to 19.53°/min in ωscan
Scan range (ω)	1.20°
Background measurement	Stationary crystal and stationary counter at beginning and end of scan, each for 25.0% of total scan time
Standard reflections	2 measured every 100 reflections
Index ranges	$0 \leq h \leq 31$, $0 \leq k \leq 33$, $0 \leq \ell \leq 5$
Reflections collected	3469
Observed reflections	2053 ($F > 6.0\sigma(F)$)
Absorption correction	Face-indexed numerical
Min/max transmission	0.0716/0.1581
	Solution and refinement
System used	Siemens SHELXTL PLUS (VMS)
Solution	Direct methods and Fourier
Refinement method	Full-matrix least-squares
Quantity minimized	$\Sigma w(\lvert F_o\rvert - \lvert F_c\rvert)^2$
Extinction correction	$x = 0.000118(7)$, where $F^* = F[1 + 0.002\,\chi F^2/\sin(2\theta)]^{-1/4}$
Weighting scheme	$w^{-1} = \sigma^2(F) + 0.000015F^2$
Number of refined parameters	153
Final R indices (obs. data)	R = 6.39%, wR = 6.73%
R indices (all data)	R = 10.73%, wR = 7.06%
Goodness-of-fit	3.19
Largest and mean Δ/σ	0.003, 0.000
Data-to-parameter ratio	13.4 : 1
Largest difference peak	4.20 e $Å^{-3}$
Largest difference hole	−3.85 e$Å^{-3}$

where r_0 = 2.541 Å for Pb–S bonds and r_0 = 2.520 Å for Sb–S bonds were chosen to obtain an electroneutral formula. The bond-valence analysis is presented in Table 6, and the derived occupation numbers are given in the last column of Table 4. The occupation numbers derived by the two methods are similar.

DISCUSSION

The distribution of lead and antimony among the cation sites in $Pb_7Sb_4S_{13}$ is complex, but the overall stoichiometry of the crystal is essentially dictated by the oxidation states of the atoms. Deviations from the nominal lead to antimony ratio will imply either sulfur vacancies or change of the oxidation states of metals. Since there is no crystallographic indication in X-ray refinement nor in the bond valence analysis for such changes, we assume the nominal composition for the compound.

The structure of $Pb_7Sb_4S_{13}$, shown in Fig. 1, consists of two types of ribbon made of back-to-back $(Pb/Sb)S_5$ square pyramids. The ribbons, shaded as parallelograms in Fig. 2, extend indefinitely in the c direction, are one pyramid thick, and have different widths. The width of the narrow ribbon (fine ruling) equals four times the basal distance of the $(Pb–Sb)S_5$ pyramid, and the width of the wide one (coarse ruling) is seven times this distance. The ribbons are arranged in a pattern identical with that in boulangerite, $Pb_5Sb_4S_{11}$ (6–8). In $Pb_7Sb_4S_{13}$, however,

TABLE 2
Atomic Coordinates and Equivalent Isotropic Displacement Parameters for $Pb_7Sb_4S_{13}$

	x	y	z	U_{eq}
M1	0.0533(2)	0.4132(2)	0.3997(15)	0.030(2)
M2	0.3968(1)	0.4964(1)	0.4158(9)	0.031(1)
M3	0.2378(1)	0.5737(1)	0.4217(10)	0.034(1)
M4	0.0783(1)	0.6515(1)	0.4288(10)	0.033(1)
M10	0.2116(2)	0.7161(1)	0.5431(17)	0.034(2)
M11	0.3744(2)	0.6368(1)	0.5602(14)	0.041(1)
M12	0.5384(1)	0.5557(1)	0.5537(12)	0.039(1)
M13	0.6841(1)	0.4676(1)	0.5614(12)	0.042(1)
M14	0.8251(1)	0.3604(1)	0.5188(9)	0.034(1)
M15	0.9881(1)	0.2981(1)	0.5279(8)	0.023(1)
M16	0.1479(1)	0.2156(1)	0.5306(8)	0.027(1)
S1	−0.0005(6)	0.6721(5)	0.9574(54)	0.025(4)
S2	0.1549(6)	0.5956(5)	0.9592(55)	0.021(3)
S3	0.3119(6)	0.5225(5)	0.9712(54)	0.024(4)
S4	0.4674(6)	0.4477(5)	0.9511(57)	0.026(4)
S5	0.6189(7)	0.3772(6)	0.9609(58)	0.035(4)
S10	0.2400(6)	0.1993(5)	0.0152(47)	0.021(3)
S11	0.0764(5)	0.2746(5)	0.0266(45)	0.017(3)
S12	0.9140(6)	0.3506(5)	0.0195(50)	0.022(3)
S13	0.7608(6)	0.4399(6)	0.0322(54)	0.027(4)
S14	0.6138(6)	0.5295(5)	0.0249(53)	0.023(3)
S15	0.4567(6)	0.6048(5)	0.0007(52)	0.028(4)
S16	0.3026(7)	0.6789(6)	0.9972(58)	0.030(4)
S17	0.1445(6)	0.7464(5)	0.0058(52)	0.024(3)

Note. $U_{eq} = (U_{11} + U_{22} + U_{33})/3$.

TABLE 3
Anisotropic Atomic Thermal Displacement Parameters ($Å^2$) for the Metal Atoms in $Pb_7Sb_4S_{13}$

	U_{11}	U_{22}	U_{33}	U_{23}	U_{13}	U_{12}
M(1)	0.0150(19)	0.0225(20)	0.0516(41)	−0.0089(24)	−0.0131(25)	−0.0010(16)
M(2)	0.0247(15)	0.0368(15)	0.0409(27)	0.0031(19)	0.0001(17)	0.0046(12)
M(3)	0.0229(13)	0.0345(14)	0.0362(24)	0.0007(17)	0.0021(17)	0.0052(11)
M(4)	0.0269(13)	0.0289(13)	0.0426(24)	0.0003(17)	0.0031(17)	0.0025(11)
M(10)	0.0240(20)	0.0213(19)	0.0586(41)	0.0082(31)	−0.0184(31)	−0.0096(16)
M(11)	0.0332(19)	0.0348(19)	0.0535(34)	−0.0018(25)	−0.0057(25)	−0.0035(16)
M(12)	0.0394(18)	0.0324(15)	0.0443(29)	−0.0041(21)	−0.0077(22)	−0.0048(13)
M(13)	0.0330(17)	0.0459(18)	0.0495(28)	0.0074(22)	0.0026(24)	−0.0103(14)
M(14)	*0.0195(11)*	*0.0534(14)*	*0.0286(19)*	*0.0078(18)*	*−0.0013(16)*	*−0.0042(11)*
M(15)	0.0246(11)	0.0215(11)	0.0225(18)	−0.0002(14)	−0.0013(15)	0.0010(9)
M(16)	0.0309(13)	0.0242(11)	0.0255(19)	0.0001(15)	−0.0022(16)	0.0034(9)

Note. The anisotropic displacement exponent takes the form $\exp[-2\pi^2(h^2a^{*2}U_{11} + \cdots + 2klb^*c^*U_{23})$.

both ribbons are wider than those in boulangerite, as shown in Fig. 2, and can be obtained by simultaneous incorporation of two PbS units into each kind of ribbon in boulangerite. Consequently, $Pb_7Sb_4S_{13}$ can be considered as a member of a boulangerite homologous series described as $Pb_{5+2n}Sb_4S_{11+2n}$, where $n = 0$ for boulangerite and $n = 1$ for $Pb_7Sb_4S_{13}$.

In agreement with the predictions of Skowron and Brown (2), the 7- and 8-coordinate sites (M14, M15, M16), where the face of one ribbon is joined to the edges of other ribbon, are fully occupied by Pb. The 5-coordinate cation sites M1 and M10, closest to the acute corners of the ribbons, are fully occupied by Sb. The rest have mixed occupancy and, because the compound is on the whole rich in lead, the mixed occupancy sites are also rich in lead relative to boulangerite.

TABLE 4
Percentage of Sb on Cation Sites in $Pb_7Sb_4S_{13}$

Site	X-ray	Bond valence method
M(1)	100	100
M(2)	28	26
M(3)	17	15
M(4)	14	12
M(10)	100	100
M(11)	65	63
M(12)	36	44
M(13)	40	40
M(14)	0	0
M(15)	0	0
M(16)	0	0
Formula	$Pb_7Sb_4S_{13}$	$Pb_7Sb_4S_{13}$

The space group symmetry of $Pb_7Sb_4S_{13}$ is lower than that of boulangerite, and the structure, unlike the previously reported lead–antimony sulfides, is noncentrosymmetric. Consequently, the mirror plane normal to the short crystallographic axis, present in most of the other lead–antimony sulfides, is lost in $Pb_7Sb_4S_{13}$. The displacement of the cations from $z = 0$ or $1/2$ is almost four times larger than that of the sulfur atoms, with the displacement of the 5-coordinate cations being larger than that of the 7- and 8-coordinate ones. The relative displacements of

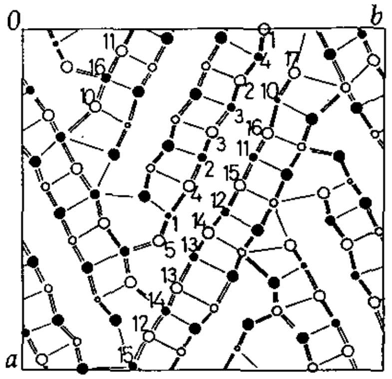

FIG. 1. The unit cell of $Pb_7Sb_4S_{13}$ projected down [001]. In order of decreasing size, the circles indicate S, Pb, mixed sites, and Sb. Atoms close to $z = 0.0$ and 0.5 are indicated by open and full circles, respectively.

TABLE 5
Interatomic Distances (Å) less than 3.7 Å in $Pb_7Sb_4S_{13}$

Narrow ribbon			Wide ribbon		
M(1)–	S(1)	2.495(14)	M(10)–	S(10)	2.149(13)
	S(5)	2.521(21)		S(17)	2.576(19)
	S(4)	2.852(19)		S(17)	2.807(20)
	S(5)	2.915(22)		S(16)	2.982(16)
	S(4)	3.154(16)		S(16)	3.228(16)
M(2)–	S(2)	2.623(14)	M(11)–	S(11)	2.520(12)
	S(3)	2.775(18)		S(16)	2.674(20)
	S(4)	2.803(19)		S(15)	2.760(18)
	S(4)	3.006(20)		S(16)	3.041(21)
	S(3)	3.090(19)		S(15)	3.099(19)
M(3)–	S(3)	2.699(14)	M(12)–	S(12)	2.618(13)
	S(2)	2.768(19)		S(14)	2.698(19)
	S(3)	2.841(18)		S(14)	2.820(19)
	S(2)	2.985(19)		S(15)	2.923(18)
	S(3)	3.118(19)		S(15)	3.211(16)
M(4)–	S(1)	2.722(19)	M(13)–	S(13)	2.672(15)
	S(4)	2.723(14)		S(13)	2.726(19)
	S(1)	2.886(19)		S(13)	2.899(20)
	S(2)	2.986(18)		S(14)	2.957(18)
	S(2)	3.146(16)		S(14)	3.167(16)
				S(5)	3.193(16)
				S(5)	3.680(16)
			M(14)–	S(12)	2.930(17)
				S(12)	2.934(17)
				S(17)	2.976(14)
				S(14)	3.116(14)
				S(10)	3.148(16)
				S(13)	3.192(16)
				S(13)	3.262(16)
				S(10)	3.323(14)
			M(15)–	S(15)	2.774(14)
				S(11)	2.966(16)
				S(11)	2.974(16)
				S(12)	2.968(17)
				S(12)	3.015(17)
				S(17)	3.378(16)
			M(16)–	S(16)	2.908(14)
				S(10)	2.959(17)
				S(10)	3.045(17)
				S(11)	3.022(15)
				S(11)	3.045(16)
				S(5)	3.158(16)
				S(5)	3.202(16)

the atoms in the narrow and the wide ribbons indicate that the ribbons are also shifted along *c* in opposite directions.

The bond-valence analysis shown in Table 6 indicates that some of the sulfur atoms are systematically overbonded (bond-valence sums larger than the atomic valence) while others are underbonded. The pattern is similar in $Pb_7Sb_4S_{13}$ and in boulangerite (8). The overbonded sulfur atoms lie close to the obtuse corners of the ribbons and bond to Pb-rich sites on the ribbon, while the underbonded ones lie close to the acute corners and bond to Sb-rich sites. Similar over- and underbonding of sulfur atoms is also present in robinsonite, $Pb_7Sb_4S_{13}$ (5) and its higher homolog $Pb_5Sb_6S_{14}$ (10) suggesting that the feature is an intrinsic property of the ribbons.

The over- and underbonding indicates respectively residual compressive and tensile stresses in the ribbons and is related to the cation distribution, as discussed by Skowron and Brown (2). The 7- and 8-coordinate Pb atoms and the 5-coordinate Sb/Pb atoms lie on opposite sides of the ribbons, and since the Pb–S bonds are longer than Sb/Pb–S bonds, there is a tendency for the ribbons to curl toward the Sb-rich side. Keeping them straight, as is required for packing, causes strain: the Pb–S bonds have to compress and the Sb/Pb–S bonds stretch. The strain on the cations is relieved by buckling the com-

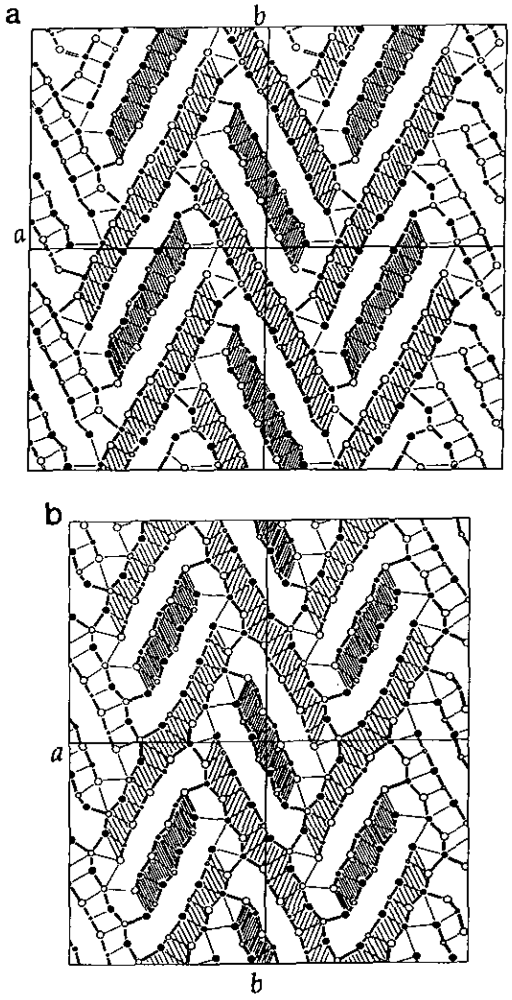

FIG. 2. Four unit cells of (a) $Pb_7Sb_4S_{13}$ and (b) boulangerite projected down [001] with the wide and narrow ribbons indicated by coarse and fine ruling. Conventions for indicating atoms are the same as in the legend to Fig. 1.

TABLE 6

Bond Valences in $PbSb_4S_{13}$ Weighted According to the X-Ray Occupation Numbers

	M1	M2	M3	M4	M10	M11	M12	M13	M14	M15	M16	
%Sb:	100	28	17	14	100	65	36	40	0	0	0	Σs
S1	1.070			1.007						0.172		−2.249
S2		0.773	0.842	0.501								−2.116
S3		0.735	1.312									−2.047
S4	0.595	0.758		0.611								−1.964
S5	1.273							0.215			0.367	−1.855
S10					1.314				0.316		0.572	−2.202
S11						1.008				0.646	0.514	−2.168
S12							0.774		0.698	0.595		−2.067
S13								1.666	0.310			−1.976
S14							1.034	0.514	0.212			−1.760
S15						0.707	0.520			0.530		−1.757
S16					0.438	0.918					0.371	−1.727
S17					1.331				0.302	0.104		−1.737
Σs	2.938	2.266	2.154	2.119	3.084	2.633	2.328	2.395	1.838	2.046	1.824	

pressed Pb side of the ribbons; i.e., the overbonded Pb atoms move outward toward the edges of the two joining ribbons and the sulfur atoms move in toward the underbonded Sb atoms on the opposite face of the ribbon. Although the buckling reduces the over- and underbonding on the Pb and Sb/Pb atoms it increases it on the sulfur atoms, in agreement with observation. In higher homologs, i.e., $Pb_7Sb_4S_{13}$ and $Pb_5Sb_6S_{14}$, where the ribbons are the wider, a second strain relief mechanism takes place: the cations move off the mirror plane thus reducing, according to the distortion theorem (9), both their own underbonding and that of the neighboring sulfur atoms.

ACKNOWLEDGMENTS

A. S. is grateful to Professor I. D. Brown for discussions and critical reading of the manuscript.

REFERENCES

1. B. Salanci, *N. Jb. Mineral. Abh.* **135,** 315 (1979).
2. A. Skowron and I. D. Brown, *Acta Crystallogr. Sect. B* **50,** (1994), in press.
3. N. Wang, *Can. Mineral.* **15,** 115 (1977).
4. "International Tables for X-Ray Crystallography," Vol IV, Tables 2.2B and 2.3, Kynoch Press, Birmingham (1974).
5. A. Skowron and I. D. Brown, *Acta Crystallogr. Sect. C* **46,** 527 (1990).
6. L. Born and E. Hellner, *Am. Mineral.* **45,** 1266 (1960).
7. I. V. Petrova, E. L. Kuznetzov, A. M. Belokoneva, E. A. Simonov, E. A. Pobedimskaya, and N. V. Belov, *Dokl. Akad. Nauk SSSR* **242,** 337 (1978).
8. A. Skowron and I. D. Brown, *Acta Crystallogr. Sect. C* **46,** 531 (1990).
9. I. D. Brown, *Acta Crystallogr. Sect. B* **48,** 553 (1992).
10. A. Skowron, I. D. Brown, and R. J. D. Tilley, *J. Solid State Chem.* **97,** 199 (1992).